EDDY WIJANTO-FILE 7

by Eddy Wijanto-file 7 Eddy Wijanto-file 7

Submission date: 14-Feb-2023 02:11PM (UTC+0700)
Submission ID: 2013878037
File name: Optical_Fiber_Technology_Journal.pdf (2.69M)
Word count: 4397
Character count: 21918

Optical Fiber Technology 60 (2020) 102385

Contents lists available at ScienceDirect

Optical Fiber Technology

journal homepage: www.elsevier.com/locate/yofte

Analysis of deep multilayer perceptron neural network in MWC coded optical CDMA system with LDPC code

Chun-Ming Huang [a,*], Chao-Chin Yang [b], Eddy Wijanto [c], Hsu-Chih Cheng [c]

[a] Department of Electronic Engineering, National Formosa University, No. 64 Wen Hua Road, Huwei Township, Yunlin County 632, Taiwan, ROC
[b] Department of Electrical Engineering, Kun Shan University, No. 195, Kunda Rd., Yongkang Dist., Tainan City 710, Taiwan ROC
[c] Department of Electro-Optical Engineering, National Formosa University, No. 64, Wenhua Road, Huwei Township, Yunlin County, 632, Taiwan, ROC

ARTICLE INFO

Keywords:
Multilayer perceptron neural network (MLPNN)
Sum-product algorithm (SPA)
Optical code-division multiple-access (OCDMA)
Low-density parity-check (LDPC) code
The stochastic gradient descent (SGD)

ABSTRACT

In this paper, applying the Deep Multilayer Perceptron Neural Network (MLPNN) to the Sum-Product Algorithm (SPA) for decoding the Modified Welch-Costas (MWC) coded Optical Code Division Multiple Access (OCDMA) system with Low-Density Parity-Check (LDPC) code is analyzed. The goal is to train the MLPNN-SPA through the stochastic gradient descent (SGD) to learn and optimize the weights to each edge of the neural network decoder. Once these parameters have been trained, the decoding complexity of the MLPNN-SPA is similar to that of the SPA. Furthermore, from the simulation results, it has been shown that the MLNN-SPA can improve the system performance without additional decoding complexity as compared to the SPA.

1. Introduction

Optical code-division multiple-access (OCDMA) techniques are getting more attractive due to multiple users can access the network asynchronously and simultaneously with a high level of transmission security. Among all OCDMA techniques, spectral-amplitude coding (SAC) can eliminate the multiple access interference (MAI) by using balanced detection [1].

In 2019, Tseng [2] utilized the cyclic ternary perfect (CTP) codes to generate one novel complementary polarization-SAC (P-SAC) schemes for free-space optics (FSO) networks. With the cyclic property of CTP codes, one compact encoder/decoder can be realized via arrayed waveguide routers. In addition, compared with previous networks, this P-SAC OCDMA-FSO network has superior spectral efficiencies.

Cheng *et al.* [3] proposed one bipolar OCDMA schemes for the wireless optical communications, which used the Walsh-Hadamard (WH) matrix to encode the polarization states of optical signals. Experimental results showed that the MAI can be completely eliminated, and it has potential for future application on the fields of high-maintenance sensor environments and environmental monitoring.

However, it has been shown that the SAC-OCDMA system capacity is mainly limited by phase-induced intensity noise (PIIN) when the signal power is relatively high. The effect of PIIN is proportional to the square of photocurrent and the electrical bandwidth of the receiver, and the system performance cannot be improved by increasing the received optical power. Several codes with ideal cross correlation ($\lambda = 1$) were proposed to reduce the influence of PIIN [4,5,6]. Since the cross correlations of Hadamard codes and CTP codes are equal or larger than 1, we adopt the Modified Welch-Costas (MWC) codes with two-code keying scheme [6] as the main OCDMA system in this paper.

Moreover, with the increasing demand for high-speed optical transmission, how to construct a OCDMA system with high performance is an important topic. Several forward-error correction (FEC) schemes had been proposed to meet the high-speed optical transmission, such as Turbo codes [7], and low-density parity-check (LDPC) codes [6,8,9]. LDPC code is a block code and can be represented by a parity check matrix H, where H is a binary matrix. The parity check matrix H is sparse, the number of non-zero element is lower compared with zero elements, which presents a character of low density [10,11]. Generally, LDPC coded schemes can significantly improve the system by increasing the code length. Its superiority has made LDPC code as error correction code recognized by IEEE in the 802.11n standard.

Recently, Deep Learning (DL) has attracted world attention due to its powerful capabilities for solving complex tasks. Several researchers attempt to decode the error correction codes by using the Neural Networks (NN). Basically, decoding can be viewed as a classification

* Corresponding author.
E-mail addresses: huangcm@nfu.edu.tw (C.-M. Huang), ccyang@mail.ksu.edu.tw (C.-C. Yang), d0777106@gm.nfu.edu.tw (E. Wijanto), chenghc@nfu.edu.tw (H.-C. Cheng).

https://doi.org/10.1016/j.yofte.2020.102385
Received 27 April 2020; Received in revised form 9 September 2020; Accepted 17 October 2020

problem, and the NN needs to learn how to classify the channel output words. The dataset used for training the NN has to include all codewords in a code space, which makes it infeasible except for very short codes.

Nachmani *et al.* [12,13,14] demonstrated that the performance of High Density Parity Check (HDPC) codes decoded by the Belief Propagation (BP) algorithm can be improved by the use of well-trained Deep Neural Networks (DNNs). This DNN decoder is constructed on the base of the Tanner graph, and it can be viewed as one weighted BP decoder because the trainable weights and bias are assigned over edges in the Tanner graph. Simulation results showed that the BER improvement was achieved by optimal training of the parameters of the neural networks. Since this weight BP decoder still satisfies the message passing symmetry conditions as the original BP decoder, the error rate is independent of the transmitted codewords while transmitting over a binary memoryless symmetric (BMS) channel [13].

Xu *et al.* illustrated the method for unfolding the structure of both Tanner and factor graphs of Polar codes and used the DNN to improve the performance of Polar codes [15]. Gruber *et al.* [16] utilized a fully connected (FC) NN to decode the random codes and structure codes. It had been shown that the decoders of structured codes are easier to learn than that of random codes, and this NN decoder has maximum a posterior (MAP) performance for very short code length.

Lian *et al.* [17] used multiple NNs to learn the relation between the signal-to-noise ratio (SNR) and the parameters in the BP algorithm for decoding the BCH code and Reed-Muller code. In [18], Kim *et al.* presented the recurrent neural network (RNN) for decoding the sequential codes, such as convolutional and turbo codes. Simulation results showed that the trained RNN architecture can decode these codes with close to optimal performance on the additive white Gaussian noise (AWGN) channel.

In this paper, we propose to use the multilayer perceptron neural network (MLPNN) to optimize the Sum-Product Algorithm (SPA) for decoding the LDPC codes in OCDMA system. The main purpose is to find the weights and bias assigning to the edges of the MLPNN-SPA to improve the system performance. For explanation, several LDPC codes of different code rates and code lengths are constructed. Simulation results show that performance improvements can be obtained by the use of MLPNN-SPA.

The rest of this paper is organize as follows. Section 2 introduces the necessary background. In Section 3, we construct several LDPC codes of different lengths and different code rates. Simulation results of the OCDMA system with these LDPC codes decoding by the MLPNN-SPA and SPA are demonstrated, respectively. Section 4 concludes the paper.

2. Preliminaries

2.1. MWC coded OCDMA system with LDPC code

In this section, we first briefly introduce the structure of MWC coded OCDMA system with LDPC code. First, the message vector u will send to the LDPC encoder to generate the codeword $\times = (x_1, x_2, \ldots, x_N)$, where N is the LDPC codeword length. Then, each of these bits is transmitted over the OCDMA system. Since the MWC coded OCDMA system can eliminate the MAI, the PIIN and thermal noise are the main noise source, and their power are denoted as $< I_{PIIN}^2 >$ and $< I_{th}^2 >$, respectively [6]. The SNR can be calculated as follows:

$$\mathrm{SNR} = I^2 / \left(< I_{PIIN}^2 > + < I_{th}^2 > \right) \tag{1}$$

It has been shown that the power calculation of $< I_{PIIN}^2 >$ and $< I_{th}^2 >$ is highly related to the noise-equivalent electrical bandwidth of the receiver and the number of active users. In addition, as shown in Fig. 1, the optical signal transmission over the OCDMA system can be viewed as transmission over one channel with Gaussian noise. The output vector at the decoder of MWC coded OCDMA system can be represented as $\mathbf{y} = (y_1, y_2, \ldots y_i \ldots, y_N)$, where $y_i = (-1)^{xi} + n_i$ for $1 \le i \le N$, where n_i is Gaussian noise with standard deviation σ_{eff}. Note that σ_{eff}^2 denotes the equivalent variance of the noise in the OCDMA system. The parameters used for constructing the MWC coded OCDMA are same as that in [6].

Finally, one iterative decoder will be used to reconstruct the message $\hat{x}$. These algorithms, which iteratively compute the distributions of variables in graph-based models, are called message passing algorithms (MPAs). SPA is one important subclass of MPAs for decoding the LDPC codes. The messages passed along the edges in this algorithm are probabilities.

Let x_i be the ith bit in a LDPC codeword $\mathbf{x}$ and y_i is the corresponding received sample. Because the MWC coded OCDMA utilized the two-code keying scheme to realize one bipolar transmission, thus, the initial log-likelihood ratio (LLR) of bits can be calculated as

$$L(x_i) = log \frac{Pr(x_i = 0 | y_i)}{Pr(x_i = 1 | y_i)} = \frac{2y_i}{\sigma_{eff}^2} \tag{2}$$

At the k-th iteration, the messages from variable nodes to check nodes are computed by:

$$L(k, q_{ij}) = L(x_i) + \sum_{j' \in C_i \backslash j} L(k-1, r_{j'i}) \tag{3}$$

where $C_i \backslash j$ denotes the set of check nodes connected to variable node x_i except check node c_j.

The messaged from check nodes to variables are updated by:

$$L(k, r_{ji}) = 2 tanh^{-1} \left(\prod_{i' \in V_j \backslash i} tanh \left(\frac{L(k-1, q_{i'j})}{2} \right) \right) \tag{4}$$

where $V_j \backslash i$ denotes the set of variable nodes connected to check node c_j except variable node x_i.

The final output variable node value for iteration k is updated as follow:

$$\hat{x}_i = L(x_i) + \sum_{j \in C_i} L(k-1, r_{ji}) \tag{5}$$

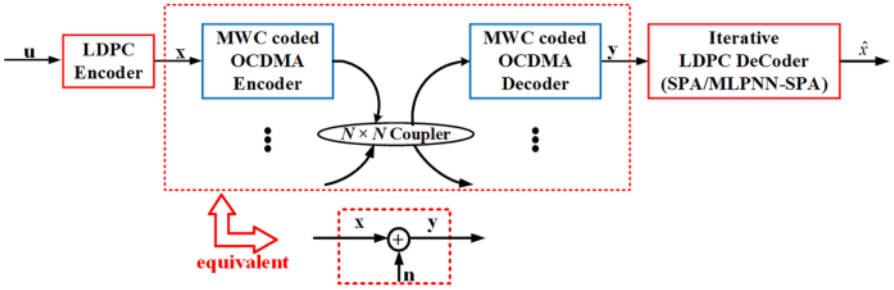

Fig. 1. System diagram of MWC coded OCDMA system with LDPC codes.

where C_i denotes the set of check nodes connected to variable node x_i.

2.2. The multilayer perceptron neural network structure

The MLPNN decoding structure are constructed by flattening the Tanner graph, where every two hidden layers corresponding to one iteration in SPA. Let P be the maximum number of iteration in SPA and E denote the number of edges in the Tanner graph. The MLPNN consists of one input layer with size N, $2P$ hidden layers with size E and one output layer with size N.

The trainable weights are assigned to the edges of the variable-to-check messages and output nodes. For odd k layer, the variable-to-check messages are updated by:

$$L(k, q_{ij}) = tanh\left(\frac{1}{2}\left(w_{k,i}L(x_i) + \sum_{j' \in C_i \backslash j} w_{k,j} L\left(k-1,\ r_{j'i}\right)\right)\right) \tag{6}$$

Note that $1 \le k \le 2P$ and $L(0, r_{ji}) = 0$ due to no information at the check nodes in the beginning. The hyperbolic tangent function was moved from check-to-variable equation to scale the messages to the reasonable range [12].

For even k layer, the check-to-variable messages are calculated by:

$$L(k, r_{ji}) = 2tanh^{-1}\left(\prod_{i' \in V_j \backslash i} L\left(k-1,\ q_{i'j}\right)\right) \tag{7}$$

Finally, the output marginalization is computed by

$$\hat{x}_i = \sigma\left(w_{2P+1,i}L(x_i) + \sum_{j \in C_i} w_{2P+1,j} L\left(2P,\ r_{ji}\right)\right) \tag{8}$$

where $\sigma = (1 + e^{-x})^{-1}$ is a sigmoid function, which is used to convert the output LLR value to the range [0,1]. If the output value is in the range (0.5, 1], it is determined to be bit 0, otherwise, bit 1.

For clarity of exposition, one (3, 3) Quasi Cyclic (QC) LDPC code based on circulant permutation matrices [19] is constructed as follows:

$$H = \begin{bmatrix} I(0) & I(0) & I(0) \\ I(0) & I(1) & I(2) \\ I(0) & I(2) & I(1) \end{bmatrix}$$

where $I(x)$ is one 3×3 identity matrix with rows cyclically shifted to the right by x positions.

Thus, this parity check matrix has code length 9. The column weight and row weight of this code are both 3 and its corresponding MLPNN structure is shown in Fig. 2. Suppose the maximum iteration number is 3, this MLPNN should have one input layer, six hidden layers and one output layer. The input (output) nodes of the first (last) is 9 and all the six hidden layers have 27 neurons corresponding to the 27 edges over its Tanner graph. The connections among these layers are determined as follow:

1. For the first (last) layer, the t-th neuron is connected to a single input node x_i in the input (output) layer if x_i is incident to edge t, where $1 \le i \le 9$ and $1 \le t \le 27$.
2. For the rest odd (even) hidden layers, the t-th neuron in this layer is connected to the neurons in previous layer, whose corresponding edges in Tanner graph are incident to $C_i \backslash j$ ($V_j \backslash i$).

Note that after the first initialization, there is no information at the check nodes, the first hidden and second hidden layer can be merged together. The self LLR message $L(x_i)$ are plotted as small arrows, as shown in Fig. 2.

Because the channel is output-symmetric, the performance of deep MLPNN-SPA decoding algorithm is independent of the transmitted codeword. Therefore, it is sufficient to use a database constructed by using the zero codeword with noise vector n to train this network. The goal is to train the weight parameters $\{w_{k,i}, w_{k,j'}, w_{k,j}\}$ to achieve the output word as close as to the zero codeword.

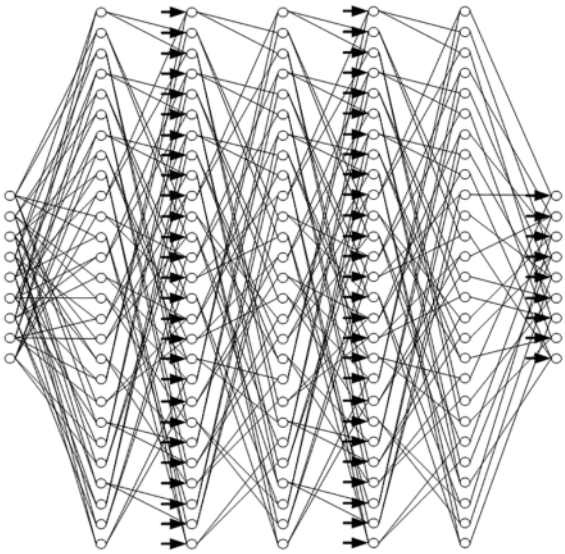

Fig. 2. Multilayer Perceptron Neural Network Architecture for (3, 3) QC-LDPC code with 3 iterations.

3. Experiments and numerical Results

The MLPNN-SPA is built in Python 3.7 and trained by using the Tensorflow library. Training was performed using the stochastic gradient descent (SGD) with mini-batches, which is the most common implementation of gradient descent in the field of deep learning. Mini-batch gradient descent attempts to find a balance between the robustness of stochastic gradient descent and the efficiency of batch gradient descent. In addition, the optimizer was adopted the RMSPROP [20] rule with different learning rates and training was done with the following cross-entropy loss function:

$$L\left(x_i, \hat{x}_i\right) = -\frac{1}{N}\sum_{i=1}^{N} x_i log\left(\hat{x}_i\right) + (1 - x_i) log\left(1 - \hat{x}_i\right) \tag{9}$$

where x_i and $\hat{x}_i$ are the ith component of the transmitted codeword and the deep neural network output, respectively.

The constructed MLPNN-SPA has 10 hidden layers, which correspond to the 5 full iterations of SPA. The training goal is to reconstruct the codeword after transmitting over the noisy channel. Each processing element in the odd (or even) layer updates the messages according to Eq. (6) (or Eq. (7)). In order to make the tanh calculation in Eq. (6) stable, similar to the SPA, it is necessary to clip the absolute value of the input to be always less than positive constant 10.

The training dataset is created by transmitting all zero codeword through the optical OCDMA system with various noise variances, which are influenced by the number of active users in the system simultaneously. Similarly, the testing dataset is created with the same way, except the codeword is randomly generated not all zero. In this paper, various QC-LDPC codes with different block lengths and rates are constructed. These LDPC codes are derived from the one-coincidence sequence (OCS) families, such as Shifted Prime (SP) Sequences and Modified Welch-Costas (MWC) Sequences [19]. For brevity, these QC-LDPC codes are named SP-OCS and MWC-OCS LDPC codes in the rest of this paper, respectively.

3.1. (3, 5) SP-OCS LDPC code with short-length

First, one SP-OCS LDPC codes with column-weight 3 and row-weight 5 is constructed. The prime modulus used for construction is $p = 31$, which yields code with length $N = 155$ and code rate $= 0.4$. The *row index sequences* (RISs) $\{m_0, m_1, m_2\}$ used for this code is $\{0, 1, 2\}$, and the *column index sequences* (CISs) $\{n_0, n_1, \ldots, n_4\}$ are $\{0, 1, 2, 3, 4\}$, respectively.

Therefore, the MLPNN-SPA consists of 10 hidden layers of size 465 ($=3 \times 155$) in this experiment. During training, the mini-batch size was set to 120 with varying active user numbers $= \{88, 80, 72, 64, 56, 48\}$ and 1000 samples per active user number. The optimizer was adopted the RMSPROP rule with learning rate 0.001 and the number of epoch is 15. Only the model with the best performance will be saved and used for decoding the non-all-zero codeword of various noise variances at the testing stage. If the performance of the testing stage is not very well, this model will be reloaded and retrained.

Fig. 3 shows the BER performance of the MWC-coded OCDMA system with (3, 5) SP-OCS LDPC code decoding by the SPA and MLPNN-SPA, respectively. Simulation results show that the BER performance of the latter is consistently smaller than that of the former. Furthermore, the coding gain for MLPNN-SPA is 0.4 dB higher than the conventional SPA with BER 9.2×10^{-8}.

3.2. (3, 8) High-rate SP-OCS LDPC code with short-length

In this experiment, one SP-OCS LDPC code with column-weight 3 and row-weight 8 is constructed. The prime modulus used for construction is $p = 31$, which yields code with length $N = 465$ and code rate $= 0.8$. The RISs $\{m_0, m_1, m_2\}$ used for this code is $\{0, 1, 2\}$, and the CISs $\{n_0, n_1, \ldots, n_{14}\}$ are $\{0, 1, 2, 3, 4, 5, 6, 7, 8, 9, 10, 11, 12, 13, 14\}$, respectively. Thus, the size of the hidden layer in the MLPNN-SPA is 1395 ($=3 \times 465$).

For training the MLPNN-SPA, the mini-batch size was set to 40 with varying two active user numbers $= \{56, 48\}$ and 3000 samples per active user number. The optimizer was adopted the RMSPROP rule with learning rate 0.001 and the number of epoch is 20. Similarly, only the model with the best performance is saved for the next testing stage.

The BER curves of the OCDMA system with (3, 8) SP-OCS LDPC code decoding by the SPA and MLPNN-SPA are depicted in Fig. 4, respectively. Similar to the (3, 5) SP-OCS code, the MLPNN-SPA achieves lower (or equal) BER performance to the SPA. At BER of 8×10^{-9}, the MLPNN-SPA outperforms the SPA about 0.3 dB.

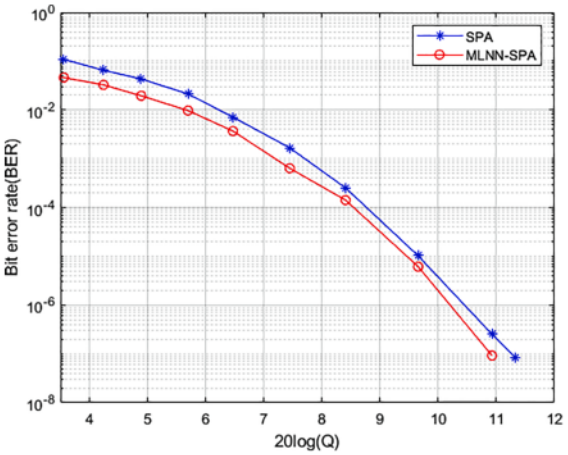

Fig. 3. BER performance of MWC coded OCDMA system with (3, 5) SP-OCS LDPC code.

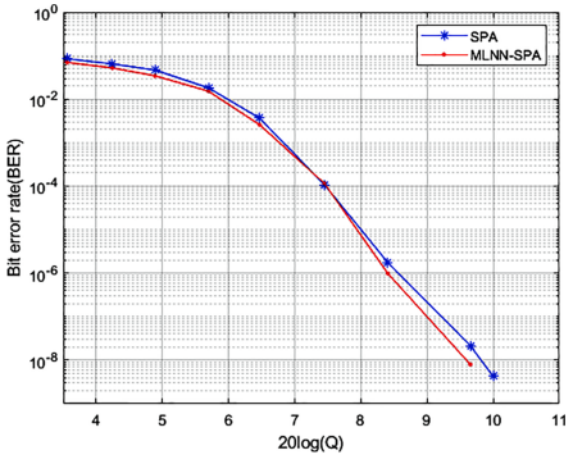

Fig. 4. BER results for MWC coded OCDMA system with (3, 8) SP-OCS LDPC code.

3.3. (4, 8) MWC-OCS LDPC codes with short- and moderate-length

Generally, the system performance can be improved by increasing the minimum distance of the LDPC codes. For a (j, k)-regular QC-LDPC code, it has been shown that the minimum distance is at most $(j + 1)!$ [21]. In addition, due to the inherent code characteristics, the MWC-OCS LDPC code has larger minimum distance that the SP-OCS LDPC code [19]. Thus, we constructed some MWC-OCS LDPC codes with column-weight 4 to observe whether the MLPNN-SPA can further obtain a lower BER than SPA.

Fig. 5 shows the performance curves for MWC-OCS LDPC codes of column-weight 4 and row-weight 8. These LDPC codes have the same code rate ≈ 0.5 but different code lengths. Since the prime numbers used to construct these codes are 31, 61 and 151, the corresponding code length N are 248, 488 and 1208, respectively. The RISs $\{m_0, m_1, m_2\}$ and CISs $\{n_0, n_1, \ldots, n_7\}$ used for these three codes are $\{29, 17, 20\}$ and $\{25, 5, 19, 7, 23, 10, 8, 13\}$, $\{1, 22, 44\}$ and $\{57, 11, 33, 14, 9, 1, 35, 20\}$, $\{79, 21, 66\}$ and $\{9, 118, 115, 18, 142, 147, 54, 71\}$.

Similarly, the MLPNN-SPA for these three codes has 10 hidden layers of different sizes (i.e., 744, 1464 and 3624, respectively). The parameters for training these MLPNNs are as follows:

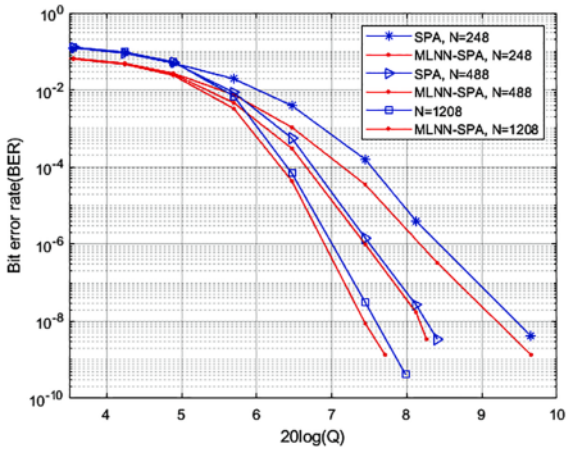

Fig. 5. BER performance of MWC coded OCDMA system with (4, 8) MWC-OCS LDPC codes.

1. For $N = 248$: The mini-batch size was set to 120 with varying active user numbers = {88, 80, 72, 64, 56, 48} and 1000 samples per active user number. The optimizer was adopted the RMSPROP rule with learning rate 0.001 and the number of epoch is 15.
2. For $N = 488$: The mini-batch size was set to 40 with varying active user numbers = {56, 54} and 3000 samples per active user number. The optimizer was adopted the RMSPROP rule with learning rate 0.001 and the number of epoch is 20.
3. For $N = 1208$: The mini-batch size was set to 20 with one active user number = {56} and 3000 samples per active user number. The optimizer was adopted the RMSPROP rule with learning rate 0.0001 and the number of epoch is 30.

Similarly, only save the model with the best performance for processing the testing stage.

As shown in Fig. 5, the MLPNN-SPA performs slightly better than the SPA for short to moderate block lengths, and it is obvious to see that the performance improves as the block length increases. For the MWC-OCS LDPC codes with code length 248 and 488, the MLPNN-SPA outperforms the SPA about 0.3 dB and 0.15 dB at BER of 10^{-9}, respectively. In addition, the MLPNN-SPA achieves coding gain of 0.15 dB over the SPA at BER of 1.3×10^{-9} for the LDPC code with code length 1208. In fact, after that point, we were not able to count any errors for at least 10^{10} bits transmitted. We believe that a much larger coding gain is expected for lower BERs.

4. Conclusion

In this paper, we applied the deep multilayer perceptron neural network techniques to the SPA for improving the performance of MWC-coded OCDMA system with LDPC codes. The aim is to train the MLPNN-SPA to learn and find the weights to each edge of the neural network decoder during the training stage. Once the weights are determined, the MLPNN-SPA is translated back to the iterative message-passing decoding as the SPA. Thus, the decoding computational complexity of the MLPNN-SPA is similar to that of the SPA.

For illustration purposes, several different OCS LDPC codes of different block lengths and rates are constructed. Simulation results show that the MLPNN-SPA achieves a lower BER performance to the SPA. Furthermore, once the parameters assigning the edges of the MLPNN-SPA have trained, the performance of MWC-coded OCDMA system can be improved without increasing computational complexity as compared to the SPA.

Declaration of Competing Interest

The authors declare that they have no known competing financial interests or personal relationships that could have appeared to influence the work reported in this paper.

References

[1] M. Kavehrad, D. Zaccarin, Optical code-division-multiplexed systems based on spectral encoding of noncoherent sources, J. Lightwave Technol. 13 (1995) 534–545.
[2] S. Tseng, A new polarization-SAC scheme suitable for compact OCDMA-FSO networks, IEEE Syst. J. 13 (2019) 1332–1335.
[3] H. Cheng, E. Wijanto, T. Lien, P. Lai, S. Tseng, Multiple access techniques for bipolar optical code division in wireless optical communications, IEEE Access 8 (2020) 83511–83523.
[4] Z. Wei, H.M.H. Shalaby, H. Ghafouri-Shiraz, Modified quadratic congruence codes for fiber Bragg-grating-based spectral-amplitude-coding optical CDMA systems, J. Lightwave Technol. 19 (2001) 1274–1281.
[5] J.F. Huang, C.C. Yang, Permuted M-matrices for the reduction of phase-induced intensity noise in optical CDMA network, IEEE Trans. Commun. 54 (2006) 150–158.
[6] J.F. Huang, C.C. Yang, C.M. Huang, On analyzing quasi-cyclic LDPC codes over modified welch-costas-coded optical CDMA system, J. Lightwave Technol. 27 (2009) 2150–2158.
[7] T. Mizuochi, Y. Miyata, T. Kobayashi, K. Ouchi, K. Kuno, K. Kubo, K. Shimizu, H. Tagami, H. Yoshida, H. Fujita, M. Akita, K. Motoshima, Forward error correction based on block turbo code with 3-bit soft decision for 10-Gb/s optical communication systems, IEEE J. Sel. Top. Quantum Electron. 10 (2004) 376–386.
[8] Y. Jinhyun, H. Jang, K. Kyoungsoo, J. Jichai, BER performance due to irregularity of row-weight distribution of the parity-check matrix in irregular LDPC codes for 10-gb/s optical signals, J. Lightwave Technol. 23 (2005) 2673–2680.
[9] B. Vasic, I.B. Djordjevic, R.K. Kostuk, Low-density parity check codes and iterative decoding for long-haul optical communication systems, J. Lightwave Technol. 21 (2003) 438–446.
[10] D.J.C. MacKay, Good error-correcting codes based on very sparse matrices, IEEE Trans. Inf. Theory 45 (1999) 399–431.
[11] R. Gallager, Low-density parity-check codes, IEEE Trans. Inf. Theory 8 (1962) 21–28.
[12] I. Be'Ery, N. Raviv, T. Raviv, Y. Be'Ery, Active deep decoding of linear codes, IEEE Trans. Commun. 68 (2020) 728–736.
[13] E. Nachmani, E. Marciano, L. Lugosch, W.J. Gross, D. Burshtein, Y. Be'ery, Deep learning methods for improved decoding of linear codes, IEEE J. Selected Top. Signal Process. 12 (2018) 119–131.
[14] E. Nachmani, Y. Be'ery, D. Burshtein, Learning to decode linear codes using deep learning, 2016 54th Annual Allerton Conference on Communication, Control, and Computing (Allerton), Allerton Park and Retreat Center, Monticello, IL, USA, 2016, pp. 341–346.
[15] W. Xu, Z. Wu, Y. Ueng, X. You, C. Zhang, Improved polar decoder based on deep learning, IEEE Int. Workshop on Signal Process. Syst. (SiPS) 2017 (2017) 1–6.
[16] T. Gruber, S. Cammerer, J. Hoydis, S.T. Brink, On deep learning-based channel decoding, 2017 51st Annual Conference on Information Sciences and Systems (CISS), Baltimore, MD, USA, 2017, pp. 1–6.
[17] M. Lian, F. Carpi, C. Hager, H.D. Pfister, Learned Belief-Propagation Decoding with Simple Scaling and SNR Adaptation. 2019 IEEE International Symposium on Information Theory (ISIT), 2019.
[18] H. Kim, Y. Jiang, R. Rana, S. Kannan, S. Oh, P. Viswanath, Communication Algorithms via Deep Learning, 2018, pp. arXiv:1805.09317.
[19] J.F. Huang, C.M. Huang, C.C. Yang, Construction of one-coincidence sequence quasi-cyclic LDPC codes of large girth, IEEE Trans. Inf. Theory 58 (2012) 1825–1836.
[20] T. Tieleman, G. Hinton, Lecture 6.5-rmsprop: Divide the gradient by a running average of its recent magnitude. COURSERA: Neural Networks for Machine Learning 4 (2012) 26–31.
[21] R.M. Tanner, D. Sridhara, A. Sridharan, T.E. Fuja, D.J. Costello Jr., LDPC block and convolutional codes based on circulant matrices, IEEE Trans. Info. Theory 50 (2004) 2966–2984.

EDDY WIJANTO-FILE 7

ORIGINALITY REPORT

12%	8%	7%	7%
SIMILARITY INDEX	INTERNET SOURCES	PUBLICATIONS	STUDENT PAPERS

PRIMARY SOURCES

1	dro.dur.ac.uk Internet Source	1%
2	rgnpublications.com Internet Source	1%
3	www.journaltocs.ac.uk Internet Source	1%
4	www.kdnuggets.com Internet Source	1%
5	Jithin Jagannath, Nicholas Polosky, Anu Jagannath, Francesco Restuccia, Tommaso Melodia. "Machine learning for wireless communications in the Internet of Things: A comprehensive survey", Ad Hoc Networks, 2019 Publication	1%
6	Huang, C.M.. "FaxWeb: accessing the WWW using the fax machine", Information and Software Technology, 19990915 Publication	1%
7	Submitted to Middle East Technical University	

	Student Paper	1%
8	Shiang-Wuu Perng, Rong-Fang Horng, Horng-Wen Wu. "Effect of a diffuser on performance enhancement of a cylindrical methanol steam reformer by computational fluid dynamic analysis", Applied Energy, 2017 Publication	1%
9	digital.lib.washington.edu Internet Source	1%
10	Ning Chen. "Parallel turbo-sum-product decoder architecture for quasi-cyclic LDPC codes", Proceedings of the 16th ACM Great Lakes symposium on VLSI - GLSVLSI 06 GLSVLSI 06, 2006 Publication	1%
11	Submitted to The Hong Kong Polytechnic University Student Paper	<1%
12	Amin Shokrollahi. "LDPC Codes: an Introduction", Coding Cryptography and Combinatorics, 2004 Publication	<1%
13	spectrum.library.concordia.ca Internet Source	<1%
14	www.upt.ro Internet Source	<1%

15	Submitted to Universiti Malaysia Perlis Student Paper	<1%
16	epdf.tips Internet Source	<1%
17	Andreas Leven, Laurent Schmalen. "Status and Recent Advances on Forward Error Correction Technologies for Lightwave Systems", Journal of Lightwave Technology, 2014 Publication	<1%
18	dds.sciengine.com Internet Source	<1%
19	Bahram Honary. "Generalized Construction of Quasi-Cyclic Regular LDPC Codes Based on Perm", 2006 IEEE International Symposium on Information Theory, 07/2006 Publication	<1%
20	Submitted to National Chung Hsing University Student Paper	<1%
21	Submitted to Universidad Nacional de Colombia Student Paper	<1%
22	Submitted to University of Birmingham Student Paper	<1%
23	eprints.bbk.ac.uk Internet Source	<1%

Exclude quotes	On	Exclude matches	< 15 words
Exclude bibliography	On		